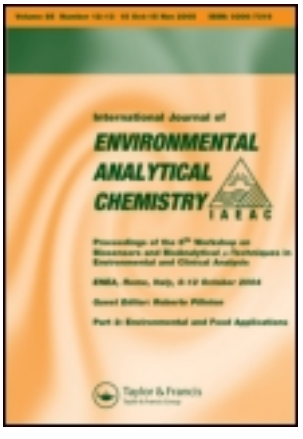

International Journal of Environmental Analytical Chemistry
Publication details, including instructions for authors and subscription information:
http://www.tandfonline.com/loi/geac20

Hydraulic modelling of horizontal-subsurface flow constructed wetlands: Influence of operation time and plant species

Javier Mena [a], José Villaseñor [b], Francisco J. Fernández [b], Rocío Gómez [c] & Antonio De Lucas [b]

[a] Research and Development Centre for Environmental Restoration (CIDRA), Alquimia Soluciones Ambientales, Polígono Industrial Daimiel Sur, 13250 Daimiel (Ciudad Real), Spain

[b] Institute of Chemical and Environmental Technology (ITQUIMA), Department of Chemical Engineering, University of Castilla-La Mancha, Avenida Camilo José Cela s/n, 13071 Ciudad Real, Spain

[c] School for Agronomical Technical Engineering (EUITA), Department of Chemical Engineering, University of Castilla La Mancha, Ronda de Calatrava s/n, 13003, Ciudad Real, Spain

Available online: 16 May 2011

To cite this article: Javier Mena, José Villaseñor, Francisco J. Fernández, Rocío Gómez & Antonio De Lucas (2011): Hydraulic modelling of horizontal-subsurface flow constructed wetlands: Influence of operation time and plant species, International Journal of Environmental Analytical Chemistry, 91:7-8, 786-800

To link to this article: http://dx.doi.org/10.1080/03067319.2010.500057

Intern. J. Environ. Anal. Chem.
Vol. 91, Nos. 7–8, 15 June–15 July 2011, 786–800

Hydraulic modelling of horizontal-subsurface flow constructed wetlands: Influence of operation time and plant species

Javier Mena[a]*, José Villaseñor[b], Francisco J. Fernández[b], Rocío Gómez[c] and Antonio De Lucas[b]

[a]*Research and Development Centre for Environmental Restoration (CIDRA), Alquimia Soluciones Ambientales, Polígono Industrial Daimiel Sur, 13250 Daimiel (Ciudad Real), Spain;* [b]*Institute of Chemical and Environmental Technology (ITQUIMA), Department of Chemical Engineering, University of Castilla-La Mancha, Avenida Camilo José Cela s/n, 13071 Ciudad Real, Spain;* [c]*School for Agronomical Technical Engineering (EUITA), Department of Chemical Engineering, University of Castilla La Mancha, Ronda de Calatrava s/n, 13003, Ciudad Real, Spain*

(*Received 25 November 2009; final version received 31 May 2010*)

Hydraulic behaviour is a very important aspect in the design of a constructed wetland (CW). Different hydraulic models have been widely applied to obtain a better understanding of CW flow properties and provide tools that optimise the design of constructed wetlands as wastewater treatments. This work studied the effects of the time of operation and the plant species used on the hydraulic characteristics of horizontal subsurface-flow (HSSF) CWs. The plug-flow with dispersion (PFD) model, the detention-time gamma-distribution (DTGD) model and a newly developed model, the multi-flow detention-time gamma-distribution (MFDTGD) model, were applied for modelling the water flow over different operating periods in five pilot-scale constructed wetlands planted with different plant species: CW1, unplanted; CW2, *Phragmites australis*; CW3, *Lythrum salicaria*; CW4, *Cladium mariscus*; and CW5, *Iris pseudacorus*. The PFD model did not provide a good fit to the experimental effluent tracer concentrations, while the DTGD model provided a satisfactory fit and the MFDTGD model, a very good fit, enabling the differentiation of several flow pathways. When using the MFDTGD model, three different types of pathways could be observed: a 'nominal' pathway, a 'tail' pathway and a 'preferential' pathway. However, the high number of parameters needed by the MFDTGD model reduces the validity of this model for use as a design tool. The values obtained for the parameters of each model were in accordance with those in previously reported studies. Regarding the effects of the operation time and the plant species, as time increased, the *N*-values tended to increase, i.e. the systems tended to behave increasingly like an ideal plug-flow reactor, especially in CWs with more developed plant species (*Iris pseudacorus* in CW5 and *Lythrum salicaria* in CW3). Globally, the CWs tended towards more homogeneous distributions of the flow, probably due to biofilm growth and plant root development.

Keywords: constructed wetland; hydraulic modelling; plant species; operation time; tracer experiment

*Corresponding author. Email: jmena@alquimiaimasd.com

ISSN 0306–7319 print/ISSN 1029–0397 online

DOI: 10.1080/03067319.2010.500057
http://www.informaworld.com

Nomenclature

CW	constructed wetland
HSSF	horizontal subsurface flow
PFD	plug flow with dispersion
DTGD	detention-time gamma-distribution
MFDTGD	multi-flow detention time-gamma distribution
HRT	hydraulic residence time [T]
t_n	nominal hydraulic residence time [T]
DTD	detention-time distribution
$E_{exp}(t)$	experimental detention-time distribution curve
M_{Tf}	recovered tracer mass [M]
Q_m	mean average flow [L^3 T^{-1}]
$\overline{t}$	mean hydraulic residence time [T]
σ_θ^2	dimensionless variance
$Q(t)$	mean flow at time t [L^3 T^{-1}]
$Q_{in}(t)$	inlet flow at time t [L^3 T^{-1}]
$Q_{out}(t)$	outlet flow at time t [L^3 T^{-1}]
W	width [L]
L	length [L]
h	height [L]
e	effective volume ratio [L^3 L^{-3}]
n	gravel porosity [L^3 L^{-3}]
V_{total}	total pore volume of CW [L^3]
V_{eff}	effective volume [L^3]
TIS	tank-in-series
D/uL	dispersion module
N	number of tanks
$E_D(t)$	detention time distribution curve of the PFD model
$E_{DTGD}(t)$	detention time distribution curve of the DTGD model
MFDM	multi-flow dispersion model
$C_{model}(t)$	tracer concentration of each model [M L^{-3}]
J	number of pathways in CW
f_i	flow fraction of the ith pathway
D/uL_i	dispersion module of the ith pathway [L^2 T^{-1}]
$\overline{t}_i$	mean hydraulic residence time of the ith pathway [T]
C_{MFDM}	tracer concentration of MFDM model [M L^{-3}]
M_{Ti}	initial tracer mass added [M]
t	time from the beginning to the sample collection [T]
$C_{exp}(t)$	experimental tracer concentration [M L^{-3}]
N_i	number of tanks of the ith pathway
C_{MFDTGD}	tracer concentration of MFDTGD model [M L^{-3}]
$\overline{t}_i/t_n$	dimensionless mean HRT
t_f	final time of the tracer experiment [T]

1. Introduction

Knowledge of hydraulic properties of constructed wetlands (CWs) is very important when these systems are designed. While idealised flow assumes that all the water and pollutant molecules have the same hydraulic residence time (HRT; also referred to as nominal hydraulic residence time, t_n), real flow means that each molecule has its own HRT [1].

The hydraulic characteristics of a CW are not constant during its operation lifetime. Also, the plant species can affect the flow behaviour [2]. Several factors such as subsurface biofilm growth [3], the accumulation of solids [4] or root development due to the presence of different kinds of plants can produce changes in flow patterns.

The flow behaviour of a CW can be expressed by a hydraulic model. Different hydraulic models have been widely applied to obtain a better understanding of CW flow and as design tools applicable to modelling CWs as wastewater treatment systems. These hydraulic models and their parameters are fitted to detention-time distribution (DTD) curves, which in turn are derived from tracer experiments.

From the tracer experiments, besides DTD, or $E_{\exp}(t)$ curves, recovered tracer masses (M_{Tf}), mean average flow (Q_m), t_n, mean hydraulic residence times ($\bar{t}$) and dimensionless variances (σ_θ^2) can be calculated for each CW using Equations (1) through (6), respectively:

$$\frac{E_{\exp}(t) = Q(t) \cdot C_{\exp}(t)}{\int_0^\infty Q(t) \cdot C_{\exp}(t) \cdot \mathrm{d}t} \tag{1}$$

$$M_{Tf} = \int_0^\infty Q(t) \cdot C_{\exp}(t) \cdot \mathrm{d}t \tag{2}$$

$$Q_m = \frac{\int_0^\infty Q(t) \cdot \mathrm{d}t}{t_f} \tag{3}$$

$$t_n = \frac{V_{\text{total}}}{Q_m} = \frac{W \cdot L \cdot h \cdot n}{Q_m} \tag{4}$$

$$\bar{t} = \int_0^\infty t \cdot E_{\exp}(t) \cdot \mathrm{d}t \tag{5}$$

$$\sigma_\theta^2 = \frac{\int_0^\infty (t - \bar{t})^2 \cdot E_{\exp}(t) \cdot \mathrm{d}t}{\bar{t}^2} \tag{6}$$

where $Q(t)$ is the average flow, obtained from the inlet and outlet flow, $Q_{\text{in}}(t)$ and $Q_{\text{out}}(t)$ respectively; $C_{\exp}(t)$ is the tracer concentration at a time t; W, L and h are the CW width, length and height respectively; n is the (gravel) bed porosity, and t_f is the final time of the tracer experiments.

In order to a better knowledge of the wetland hydraulics, Persson and Wittgren [5] introduced a new parameter, the effective volume ratio (e), which represents the volume fraction of the CW volume that is utilised for flow. It can be calculated by Equation (7), where V_{total} is the total pore volume of the CW and V_{eff} is the effective volume as calculated by Equation (8):

$$e = \frac{V_{\text{eff}}}{V_{\text{total}}} = \frac{\bar{t}}{t_n} \tag{7}$$

$$V_{\text{eff}} = Q_m \cdot \bar{t} \tag{8}$$

Different hydraulic models, calculated from the characteristic parameters of the DTD curves (σ_θ^2 and $\bar{t}$), are used to obtain an easy design tool. The most common hydraulic models applied to the DTD curves are the plug-flow with dispersion (PFD) model and the tank-in-series (TIS) model. The latter is a special case of the detention-time gamma-distribution (DTGD) model [6], which assumes that the water molecules have a gamma-distribution of HRT values. The DTGD and TIS models usually provide better fittings to the DTD data than the PFD model [7]. These models can be calibrated by obtaining the values of the different parameters: the dispersion module (D/uL) for the PFD model by using Equation (9), when D/uL is higher than 0.05 [8], and the 'number of tanks' (N) for the DTGD model by using Equation (10). With these parameter values, the theoretical $E_{\text{model}}(t)$ curves can be calculated as ($E_D(t)$) for the PFD model and ($E_{\text{DTGD}}(t)$) for the DTGD model with Equations (11) and (12), respectively, where $\Gamma(N)$ is the Γ function of N and is expressed by Equation (13) [9]. When N is an integer, the Γ function is $\Gamma(N) = (N-1)!$, and, when $N = 1$, the gamma-distribution becomes the exponential distribution. The theoretical tracer concentrations predicted by each model ($C_{\text{model}}(t)$) can be calculated with Equation (14) by introducing the respective $E(t)$ curves.

$$\sigma_\theta^2 = 2\frac{D}{uL} + 8\left(\frac{D}{uL}\right)^2 \tag{9}$$

$$N = \frac{1}{\sigma_\theta^2} \tag{10}$$

$$E_D(t) = \frac{e^{-\frac{\left[1-\left(\frac{t}{\bar{t}}\right)\right]^2}{4\cdot\left(\frac{D}{uL}\right)\cdot\left(\frac{t}{\bar{t}}\right)}}}{2\cdot\bar{t}\cdot\sqrt{\pi\cdot\left(\frac{D}{uL}\right)\cdot\left(\frac{t}{\bar{t}}\right)}} \tag{11}$$

$$E_{DTGD}(t) = \frac{N}{\bar{t}\cdot\Gamma(N)}\left(\frac{N\cdot t}{\bar{t}}\right)^{N-1}\cdot\exp\left(-\frac{N\cdot t}{\bar{t}}\right) \tag{12}$$

$$\Gamma(N) = \int_0^\infty t^{N-1}\cdot e^{-t}\cdot \mathrm{d}t \tag{13}$$

$$C_{\text{model}}(t) = \frac{E_{\text{model}}(t)\cdot M_{Tf}}{Q_m} \tag{14}$$

Researchers have applied some different hydraulics models. For example, Maloszewski *et al*. [2] developed the multi-flow dispersion model (MFDM) which divided the total flow into a number, J, of different flow fractions, f_i, that followed different pathways, each one with its own hydraulic features, and applied the PFD model to all of them, obtaining different dispersion modules (D/uL_i) and mean HRT ($\bar{t}_i$) values. The sum of all the flow fractions at the system outlet resulted in the total flow, obtaining the theoretical tracer concentrations predicted by the model (C_{MFDM}) which can be fitted to the experimental tracer data. The MFDM model is presented schematically in Figure 1.

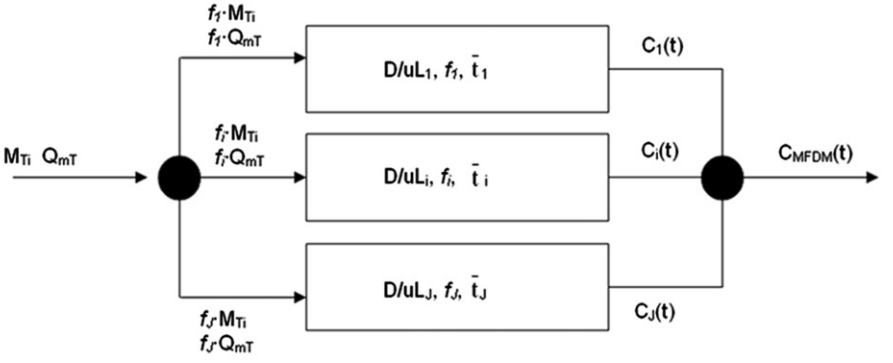

Figure 1. Conceptual diagram of the MFDM model [2].

In the present work, a new model considering the 'multi-flow' proposal was developed and used, but applying the DTGD model to each flow fraction, which usually results in better fittings than the PFD model [7]. This model was named the multi-flow detention-time gamma-distribution (MFDTGD) model.

The aim of this work was to study the influence of the operational period and the particular plant species on the hydraulics of horizontal-subsurface (HSSF) CWs through the application of the two common hydraulic models (PFD and DTGD) and a multi-flow hydraulic model (the MFDTGD model). An evaluation of the most accurate model is presented in this paper.

2. Experimental

2.1 *The experimental installation*

The experimental pilot-scale system that served as the basis of this study was situated on a farm near Ciudad Real, in southern Spain (Figure 2). The installation consisted of a synthetic domestic wastewater-feeding system, five HSSF CWs and a system for purified-wastewater collection. The feeding system consisted of a 1.5 m^3 water tank (a) with temperature control (b), a 50 litre concentrated wastewater tank (d) and two peristaltic pumps (c and e) to feed the 20 litre mixing tank (f) with (tap) water and the concentrated wastewater; five additional peristaltic pumps (g) continuously fed the parallel wetlands. The wetlands consist of five experimental 2.5 m × 0.65 m channels (h) with a bed depth of 0.6 m, situated on a covered platform in order to protect them from the rain, with a longitudinal slope of 1%. A different species of macrophyte was planted in each wetland except for wetland 1, which was used as a control without plants. The distribution of species was as follows: CW1: control; CW2: *Phragmites australis* (reed); CW3: *Lythrum salicaria* (purple loosestrife); CW4: *Cladium mariscus* (sedge); and CW5: *Iris pseudacorus* (yellow flag). All the CWs were filled with gravel with a particulate diameter of 6–9 mm, apart from two 10 cm layers located at the influent distribution and effluent collection zones, for which the particulate diameter was 9–12 mm to improve the distribution of wastewater in the CW. There were sample points (i) located throughout the CW and the effluent was conducted into a collecting system (j).

The selection of the plant species was carried out following different aspects. The reed was chosen because it is the more common and studied in wastewater treatment with CWs.

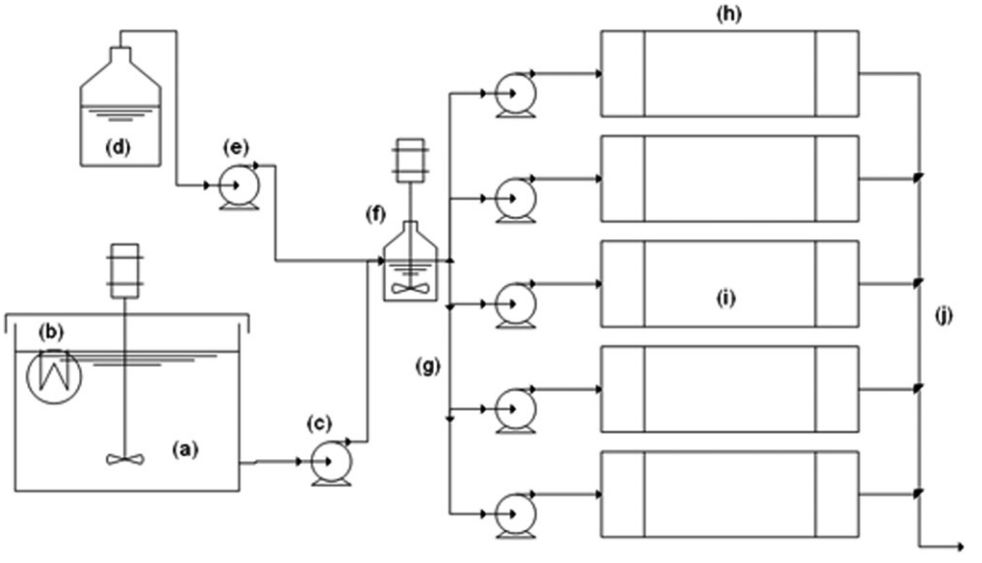

Figure 2. Diagram of the experimental installation.

The other ones were chosen according to the high biomass rate [10] or if it was autochthonous of Castilla-La Mancha [11]. For example, the sedge is very common in Castilla-La Mancha and the greater plant group of this species in Europe is located in Daimiel, i.e. 'Tablas de Daimiel' [11].

2.2 *Operating conditions*

The synthetic wastewater simulated a low-loading domestic physically pre-treated wastewater, and was prepared as previously described [12]. The average concentrations of the measured parameters of the wastewater entering the wetlands are shown in Table 1 and its composition in terms of its main components is shown in Table 2.

The CWs were continuously fed, keeping the operating conditions constant: control temperature in the well tank, 25°C; inlet flow in each wetland, 40 L d^{-1}; and mean surface organic loading, 4.8 g COD d^{-1} $m^{-2}_{surface}$.

2.3 *Tracer experiments*

Three groups of tracer experiments were carried out in all the CWs on different days of operation. The first group included only one experiment, and was carried out during the start-up of the wetlands ($t = 0$) exclusively on CW1 (Experiment 1.1), prior to feeding wastewater to the system. Then, all the CWs were continuously fed with synthetic wastewater. A second group of simultaneous tracer experiments was carried out after eight months of continuous operation in all the CWs (Experiments 2.1 to 2.5), and, finally, the last group of simultaneous tracer experiments was carried out after 24 months of continuous operation in all the CWs (Experiments 3.1 to 3.5). The 11 tracer experiments were carried out following the methods proposed by García *et al.* [13].

Table 1. Average inlet wastewater parameters.

Parameters	Concentration ($mg\,l^{-1}$)
Total COD	197
Total BOD_5	101
Soluble COD	104
Soluble BOD_5	78
TSS	117
TN	16
TKN	14.5
NH_4^+-N	9
NO_3^--N	1.5
TP	2.9
PO_4^{3-}-P	1.9
SO_4^{2-}	160

Table 2. Average inlet wastewater composition.

Components	Concentration ($mg\,l^{-1}$)
Sugar	153
Powder milk	60
Na_2CO_3	25
K_2HPO_4	10
$MgSO_4 \cdot 7H_2O$	1.5
$FeCl_3 \cdot 6H_2O$	2.5
KCl	2
$(NH_4)_2SO_4$	66

The experiments consisted of injection of a bromide solution at the CW inlets. The measurement bromide concentrations were then measured over several days at the CW outlets. One litre of a sodium bromide solution (5000 mg L^{-1}, except in Experiment 1.1, which was 10000 mg L^{-1}) was fed as a single pulse in each CW, so the total tracer mass initially added (M_{Ti}) was 5000 mg. After the pulse, the wastewater feeding was kept continuous and effluent samples were collected over time (t). Moreover, before each collection, $Q_{in}(t)$ and $Q_{out}(t)$ were measured. The frequency of the sample collection was variable and was maximised at times close to t_n; sample collection ended at a time approximately equal to three times the t_n value. The bromide concentration of each sample was measured by ion chromatography using an 'IC Metrohm' chromatograph with a 'Metrosep Anion Dual 2' anionic column and a conductivity detector with suppression.

2.4 *Modelling*

Once $C_{exp}(t)$ was measured in each experiment, DTD curve and its characteristic parameters, $\bar{t}$ and σ_θ^2, were calculated by applying Equations (1), (5) and (6), respectively.

Also, M_{Tf}, Q_m, t_n and e were calculated with Equations (2), (3), (4) and (7), respectively. These results were previously presented and discussed in Mena *et al.* [14].

The PFD and DTGD models were calibrated and their parameters were calculated for each CW: D/uL for the PFD using Equation (9) and N for DTGD using Equation (10). With these values, the $E_D(t)$ and the $E_{DTGD}(t)$ theoretical curves were calculated using Equations (11) and (12), respectively. Finally, the theoretical tracer concentration curves predicted by the models were calculated using Equation (14) and compared to the experimental tracer concentration curves.

Taking into account the experimental data, where several tracer peaks were observed, possibly indicating the presence of preferential pathways, a new model similar to the MFDM proposed by Maloszewski *et al.* [2] was proposed, as previously described. In contrast to these authors, the new model used the DTGD model instead of the PFD model to describe the multiple flow fractions in the wetland. Thus, this model was named the multi-flow detention-time gamma-distribution (MFDTGD) model. Therefore, N_i values were calculated instead of D/uL_i; the remaining parameters were calculated in the same way.

This model has a large number of parameters: the number of flow fractions (J) and, for each one, the fractional value (f_i) and the corresponding N_i and $\bar{t}_i$ values. It was assumed that all systems can be divided into a maximum of six flow fractions ($J=6$), but in the calculations, the J-value never exceeded five. These parameters were calculated using the Solver tool of the Excel program, which uses the 'generalised reduced-gradient' (GRD2) algorithm for non-linear problems and the 'Simplex' method for linear problems [15].

From the DTD curves of each experiment, the theoretical outlet tracer concentration given by this model can be calculated using Equation (15):

$$C_{\mathrm{MFDTGD}}(t) = \frac{M_{Tf}}{Q_{mT}} \cdot \sum_{i=1}^{J} \left(\frac{N_i}{\bar{t}_i}\right)^{N_i} \cdot \exp\left(-\frac{N_i \cdot t}{\bar{t}_i}\right) \cdot \frac{t^{N_i-1}}{\Gamma(N_i)} \cdot f_i \tag{15}$$

3. Results and discussion

3.1 *Modelling DTD with PFD and DTGD*

Table 3 shows the D/uL values of the PFD model, the N-values of the DTGD model and the regression coefficient of each model fitting (in parentheses) in all the experiments. As an example, Figure 3 shows the fitting of the PFD and DTGD models to the experimental tracer data in CW2 and CW5: Experiments 2.2, 2.5, 3.2 and 3.5, respectively.

All the tracer curves presented an asymmetric Gaussian distribution with a long, skewed tail, which has also been observed in other studies [16,17] and made the experimental HRT higher than the nominal one [12]. The presence of these tails could be due to presence of dead zones, stagnant zones, backflows [1] or adsorption of the tracer by the gravel [18].

Ascuntar *et al.* [18] used Rhodamine WT in a tracer test, obtained mass recoveries between 61 and 91% with an average value of 75% and evidenced that tracer adsorption was a plausible reason to make the experimental HRT higher than the nominal one. On the other hand, bromide was used in the present work obtaining mass recoveries between 76 and 94% with an average value of 83% [12]. This fact agrees with other

Table 3. Parameter values obtained from the fittings of PFD and DTGD models.

Experiment	CW	D/uL	N
Group 1 ($t=0$, wetlands start up)			
1.1	1	0.2054 (−0.117)	2.43 (0.769)
Group 2 ($t=8$ months)			
2.1	1	0.1873 (0.402)	2.67 (0.914)
2.2	2	0.3095 (0.180)	1.62 (0.656)
2.3	3	0.1661 (0.116)	3.01 (0.733)
2.4	4	0.1529 (0.873)	3.27 (0.962)
2.5	5	0.1429 (0.339)	3.50 (0.863)
Group 3 ($t=24$ months)			
3.1	1	0.1088 (0.218)	4.59 (0.720)
3.2	2	0.3418 (0.121)	1.46 (0.519)
3.3	3	0.1025 (0.131)	4.88 (0.714)
3.4	4	0.1714 (−0.404)	2.92 (0.466)
3.5	5	0.1000 (0.551)	5.00 (0.861)

Note: In parentheses: regression coefficient.

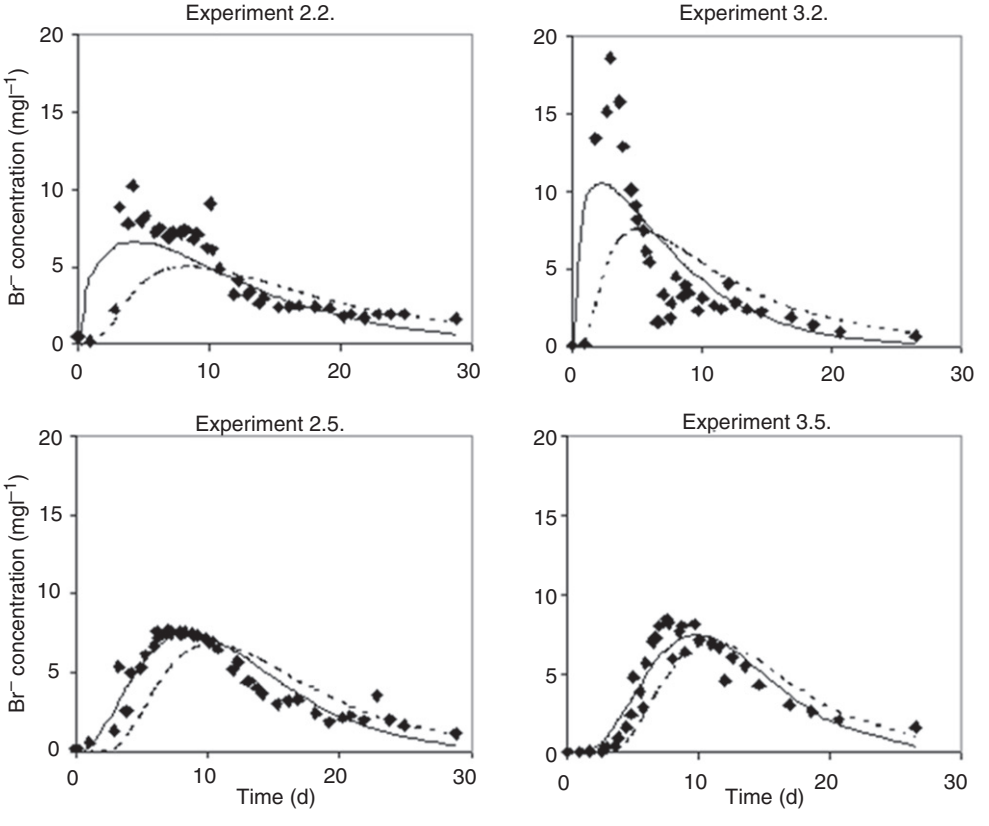

Figure 3. Fitting of the PFD (····) and DTGD (——) models to the experimental tracer concentrations (◆).

publications that demonstrated that bromide has low adsorption [19,20] and less than Rhodamine WT [21]. Although bromide has higher mass recoveries, it does not mean that there is not adsorption. Adsorption depends on the concentration. At high concentrations bromide can be adsorbed and, when fresh water passes, it can be released slowly increasing the experimental HRT. So, the influence of the adsorption on the tracer behaviour is little but can not be neglected.

Although the D/uL values were high in all the CWs ($D/uL > 0.1$), they agreed with the values commonly obtained in HSSF CWs, e.g. Bavor *et al.* [22] reported a value of 0.11 for the dispersion module or Ascuntar *et al.* [18] a values between 0.05 and 0.16. Some N-values published in literature were in the range of 1 to 8 tanks in series [6] or 4 to 11 [18], while in the present experiments they were between 1.5 and 5.

As mentioned, the DTD curves exhibited long skewed 'tails' (Figure 3) suggesting the presence of dead zones, tracer adsorption or preferential pathways, meaning that there were likely multiple flow channels and perhaps unrealistically large dispersion modules [23]. Based on the results in Figure 3 and the values of the regression coefficients in Table 3, the PFD model can be considered inadequate for the modelling of this kind of system due to the poor fit to the experimental data. This poor fit could be caused by the long skewed 'tail', which increased the mean HRT, causing a lag in the PFD predictions in relation to the experimental data. Also, the PFD model assumes that the flow acts as an ideal plug flow with a certain degree of inter-mixing, the magnitude of which is independent of the position inside the wetland. This feature means that there are no dead zones and deviations or fluid short-circuiting in the wetland considered in the PFD model. The poor fit of this model to the experimental data implies the presence of dead zones or preferential pathways.

The DTGD model fitted the experimental tracer-concentration data satisfactorily and also the accumulated mass of the tracer. This model is simple, workable, without complex program requirements and simulates the experimental data very well.

Taking into account the superior fit of the DTGD model, the influences of the operation time and the plant species will be discussed based only on the differences in the N-values. The N-value gives an idea of how closely the system approaches an ideal plug flow. The higher N is, the closer the CW and the ideal system will be. As an approximate tendency, it can be observed that N-values increased at longer operating times, except for the CW2 and CW4, which decreased slightly. This increase could evidence a correction of the possible deviations from the ideal flow; this behaviour has been observed previously [2]. The biofilm growth after several months of wastewater treatment could modify the existence of preferential pathways, closing some of them and opening others, although, generally, the flow tended towards a more homogeneous distribution. This suggests that the biofilm growth could regulate the flow distribution. Moreover, a modification of the hydraulic conductivity and a compression of the gravel can occur [7,24]. This explanation is valid only when the size of the preferential pathways is relatively small. When these pathways have a larger pore size, the biofilm growth can not correct the hydraulic defects. This last fact could occur in CW2, which was less close to the ideal plug flow. Ascuntar *et al.* [18] obtained apparent opposite conclusions related to the influence of the operation time to the dispersion. They reported that the dispersion module increased as the operational time progressed and argued that the plants development increases the micro-mixing zones and, in turn, the death zones. This fact is not opposite to the argument of the present work, i.e. the regulation with the time of the preferential pathways by the biofilm growth. They can be complementary. Both facts can occur as

Table 4. Approximate data and qualitative information regarding plants growth.

	Plants	Height (m) at the end of the experiments	Wetland surface covered by plants at the end (%)	General growth observed
HSSF CW1	No plants	–	–	–
HSSF CW2	*Phragmites australis*	1,0	50	Good
HSSF CW3	*Lythrum salicaria*	1,4	60–70	Good
HSSF CW4	*Cladium mariscus*	0,3	<5	Poor
HSSF CW5	*Iris pseudacorus*	1,5	>80	Very good

time goes by and, depending on which effect is bigger, the dispersion will increase or decrease.

Table 3 also shows differences between the five CWs in a unique group of experiments. These differences would be due to the different plant species; indeed, the differences between wetlands were higher in the last group, when more developed plants were present. This effect may be because each plant species has characteristic roots, root depth differs among them and biofilm growth will be more favoured by some than others, depending on the oxygen supply and the root density. While plant growth increases the dispersion in surface flow CWs [25], in subsurface-flow CWs the presence of plants [16] and biofilm growth [3] both decrease dispersion. In a previous work [26], results of plant development (height, wetland surface covered by the plant and general growth observation) were studied and are shown in Table 4. In the present work, in contrast to other studies [18,27] that affirmed that the presence of more root density increased the retention of the tracer causing death zones, it seems that the plants with more growth and density, especially purple loosestrife (CW3) and yellow flag (CW5) [12], contributed to a homogenisation of the flow, as discussed previously. Because of this homogenisation, these systems obtained higher *N*-values and hence, flows closer to the ideal plug flow. Also, these more developed species obtained higher values of oxygen release rate and higher values of oxidation-reduction potential inside the wetland [26], favouring the biofilm growth and hence the previously commented effect: correction of the preferential pathways by the biofilm growth.

3.2 *Modelling using the multi-flow detention-time gamma-distribution (MFDTGD) model*

In Table 5, the parameter values of the MFDTGD model after the fitting to each experiment are shown; in Table 6, the regression coefficients of each fitting are shown.

Figure 4, as an example, shows the fitting of the MFDTGD model to Experiments 2.2, 2.5, 3.2 and 3.5. The MFDTGD model obtained very good fittings to the experimental data, as corroborated by high values of the regression coefficients, shown in Table 6. The model provides a wide perspective of the flow inside each system although its high number of parameters reduces the validity of this model for use as a design tool.

Table 5 and Figure 4 show three different types of flow pathways; Figure 4d represents the first one (i), the 'nominal pathway' (listed in bold type in Table 5), which was characterised by a $\bar{t}_i$ very similar to the t_n of the CW, a high flow fraction and a relatively

Table 5. Parameters of the MFDTGD model in all the experiments.

		Group 1 (Experiment 1.1)				Group 2 (Experiments 2.1. to 2.5)				Group 3 (Experiments 3.1. to 3.5)			
		f_i	N_i	$\overline{t}_i$ (d)	$\overline{t}_i/t_n$	f_i	N_i	$\overline{t}_i$ (d)	$\overline{t}_i/t_n$	f_i	N_i	$\overline{t}_i$ (d)	$\overline{t}_i/t_n$
CW1	Pathway 1	**0.56**	**5.28**	**7.3**	**0.77**	0.05	65.44	3.6	0.37	0.04	8.34	2.8	0.28
	Pathway 2	0.44	9.72	20.8	2.17	**0.34**	**5.20**	**8.8**	**0.90**	0.17	40.36	6.0	0.61
	Pathway 3	–	–	–	–	0.60	2.03	13.4	1.37	0.09	98.56	8.4	0.85
	Pathway 4	–	–	–	–	–	–	–	–	**0.19**	**27.92**	**11.7**	**1.18**
	Pathway 5	–	–	–	–	–	–	–	–	0.52	7.24	17.1	1.73
CW2	Pathway 1	–	–	–	–	0.13	23.21	4.0	0.44	**0.60**	**5.40**	**3.6**	**0.37**
	Pathway 2	–	–	–	–	**0.40**	**8.17**	**7.6**	**0.84**	0.03	99.48	8.8	0.90
	Pathway 3	–	–	–	–	0.05	99.01	10.0	1.11	0.37	7.13	15.4	1.58
	Pathway 4	–	–	–	–	0.43	5.50	19.1	2.13	–	–	–	–
CW3	Pathway 1	–	–	–	–	0.07	97.98	3.4	0.35	0.04	19.27	4.0	0.44
	Pathway 2	–	–	–	–	0.07	99.65	4.5	0.46	0.03	97.32	6.3	0.70
	Pathway 3	–	–	–	–	**0.58**	**8.40**	**8.6**	**0.88**	**0.77**	**4.45**	**11.3**	**1.26**
	Pathway 4	–	–	–	–	0.28	10.50	19.0	1.94	0.16	31.49	15.8	1.75
CW4	Pathway 1	–	–	–	–	0.01	98.74	3.4	0.39	0.08	71.45	3.2	0.34
	Pathway 2	–	–	–	–	**0.59**	**4.96**	**8.7**	**1.00**	**0.41**	**6.96**	**5.9**	**0.61**
	Pathway 3	–	–	–	–	0.40	6.38	20.6	2.37	0.04	98.98	8.8	0.92
	Pathway 4	–	–	–	–	–	–	–	–	0.47	11.88	15.6	1.62
CW5	Pathway 1	–	–	–	–	0.02	95.60	3.3	0.31	0.03	96.53	5.2	0.54
	Pathway 2	–	–	–	–	**0.75**	**5.08**	**9.9**	**0.91**	0.07	98.21	7.0	0.73
	Pathway 3	–	–	–	–	0.02	99.25	16.2	1.50	**0.35**	**14.08**	**10.1**	**1.06**
	Pathway 4	–	–	–	–	0.21	28.83	23.4	2.16	0.65	4.19	18.8	1.96

Note: In bold: Nominal pathway.

Table 6. Regression coefficients of the MFDTGD model of each fitting.

CW	Group 1	Group 2	Group 3
1	0.9065	0.9788	0.8691
2	–	0.9098	0.9424
3	–	0.9386	0.9681
4	–	0.9894	0.9298
5	–	0.9471	0.9417

low dispersion. The second one (ii), denoted the 'tail pathway', was characterised by a high $\overline{t}_i$, a high flow fraction and a very high dispersion; the last one (iii), referred to as the 'preferential pathway', was characterised by a low $\overline{t}_i$, a low flow fraction and a very low dispersion.

Pathway (i) represents the normal flow of the tracer through the gravel of the CW. Pathway (ii) forms the final tail of the tracer and, hence, represents the dead zones that can occur in the CWs. Finally, pathway (iii) represents the preferential pathway of flow through the CW; there can be several pathways of this last type.

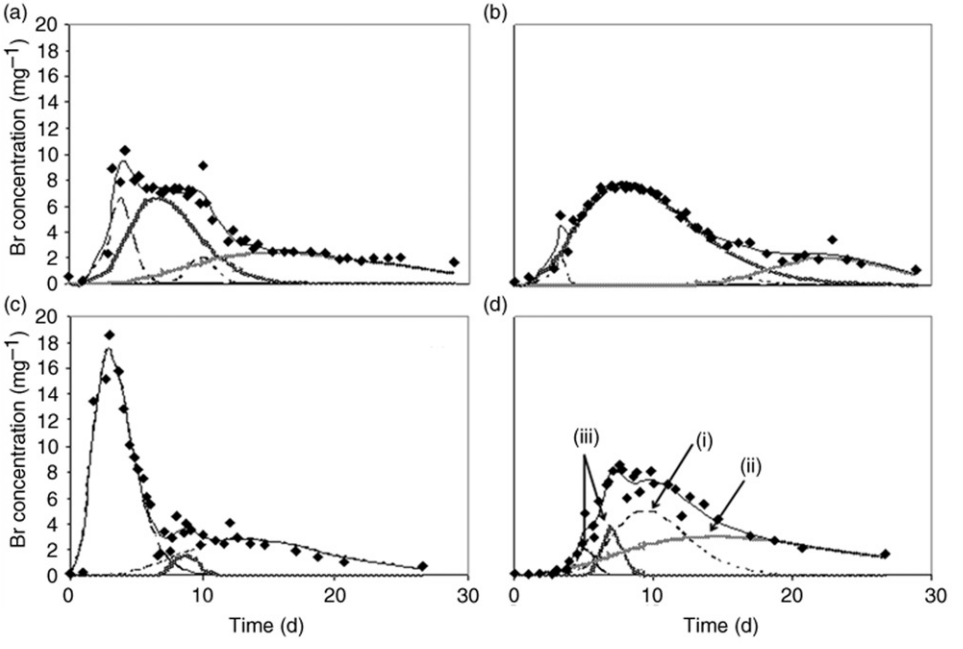

Figure 4. Fitting of the MFDTGD (——) model to the experimental tracer concentrations (◆) of experiments 2.2 (a), 2.5 (b), 3.2 (c) and 3.5 (d), by different pathways: 1 (-·-·), Pathway 2 (▫▫▫▫▫▫), Pathway 3 (- - - -), Pathway 4 (▪▪▪▪▪▪).

As operating time increased, the unplanted CW1 reached five possible pathways instead of two larger ones, which tended to make the flow more homogeneous, a fact that agrees with the previous argument regarding the increase in the stability of the system with operating time (Table 5). With respect to the planted CWs, there was no clear tendency of either increase or decrease of the flow fractions. It was not certain that the pathways found in different CWs with the same $\bar{t}_i$ were also the same because the mean HRTs could not be directly compared due to the different average operating flows. Due to this inherent difference, a dimensionless mean HRT ($\bar{t}_i/t_n$) was calculated for each flow in order to compare the pathways from different experiments. This parameter relates the mean HRT of each pathway with the HRT that it would have if the system acted as an ideal plug-flow reactor; these values are also shown in Table 5.

CW2 and CW4, which obtained the lowest *N*-values of the DTGD model, had dimensionless mean HRTs of the nominal pathways far from unity, meaning that in these CWs there were other effects that caused deviation of the flow from ideal plug flow. Because of the $\bar{t}_i/t_n$ values less than 1, this effect was likely the presence of preferential pathways. The other CWs obtained $\bar{t}_i/t_n$ values very close to 1, and it can also be observed that the greater the f_i of the nominal pathway was, the lower the *N*-value of this pathway was. This means that if the pathway represents a greater fraction of the flow, it will display more dispersion and less ideality. Conversely, if the model allowed for an infinite number of pathways with infinitesimal flow fractions, the *N*-value would also be infinite.

With respect to the preferential pathways, as operating time increased, the f_i of these pathways generally decreased. This fact supports the previous arguments: the expected

biofilm growth along with plant development would regulate the flow distribution, closing preferential pathways due to the higher biofilm growth in these zones because the microorganisms would have more access to nutrient supply due to the increased turbulence.

With respect to the tail pathways, comparing the results in groups 2 and 3 it can generally be observed that the dimensionless HRT decreased in the planted CWs. This suggests that the plant development reduced the dead zones, although the f_i evolution did not present a clear tendency.

4. Conclusions

The PFD model provided a poor fit to the experimental effluent tracer concentrations, while the DTGD yielded a satisfactory fit, and the MFDTGD model gave a very good fit, enabling the differentiation of several flow pathways, although the large number of parameters in the MFDTGD model reduces the validity of this model for use as a design tool. When using the MFDTGD model, three different types of pathways could be observed: a 'nominal' pathway, a 'tail' pathway and a 'preferential' pathway. With this new model, the person in charge of the operation and maintenance can know how his wetland is functioning and detect the possible hydraulic defects to solve them faster. It is impossible to know how many preferential pathways a wetland is going to have before its construction. So, more research is needed in order to determinate if it is any relation between the gravel features, the collocation form of that gravel, the form of the wetland (Length to Width ratio) or the depth for example.

The values obtained for the parameters of all models were in accordance with previously reported works [6,18,22]. Regarding the effect of the operating time and the plant species, as time increased, the *N*-values tended to increase, i.e. the systems tended to behave increasingly like an ideal plug-flow reactor, especially in the CWs with more developed plant species (*Iris pseudacorus* in CW5 and *Lythrum salicaria* in CW3). Generally, the CWs tended towards more homogeneous distribution of the flow, probably due to the biofilm growth and root development of the plants.

References

[1] O. Levenspiel, *Chemical Reaction Engineering*, 3rd ed. (John Wiley & Sons, New York, USA, 1999), p. 668.
[2] P. Maloszewski, P. Wachniew, and P. Czuprynski, J. Hydrol. **331**, 630 (2006).
[3] F. Suliman, H.K. French, L.E. Haugen, and A.K. Søvik, Ecol. Eng. **27**, 124 (2006).
[4] A. Caselles-Osorio, J. Puigagut, E. Segú, N. Vaello, F. Granés, D. García, and J. García, Water Res. **41**, 1388 (2007).
[5] J. Persson and H.B. Wittgren, Ecol. Eng. **21**, 259 (2003).
[6] R.H. Kadlec, Ecol. Eng. **20**, 1 (2003).
[7] R.H. Kadlec and R.L. Knight, *Treatment Wetlands* (CRC Press, Boca Raton, Florida, 1996), p. 893.
[8] O. Levenspiel and W. Smith, Chem. Eng. Sci. **6**, 227 (1957).
[9] H.B. Dwight, *Tables of Integrals and Other Mathematical Data* (Macmillan, New York, 1961), p. 336.
[10] S.L. Emery and J.A. Perry, Am. Midl. Nat. **134**, 394, (1995).

[11] S. Cirujano, *Plantas Acuáticas de las lagunas y humedales de Castilla-La Mancha* (Ilustraciones Marta Chirino Argenta, Spain, 2002) [In Spanish].
[12] J. Villaseñor, A. De Lucas, R. Gómez, and J. Mena, Environ. Technol. **28**, 1333 (2007).
[13] J. García, E. Ojeda, E. Sales, F. Chico, T. Píriz, P. Aguirre, and R. Mujeriego, Ecol. Eng. **722**, 1 (2003).
[14] J. Mena, R. Gómez, J. Villaseñor, and A. De Lucas, presented at the 11th International Conference on Wetland Systems for Water Pollution Control (IWA), Indore, India, 2008 (unpublished).
[15] D. Fylstra, L. Lasdon, A. Warren, and J. Watson, Interfaces **28**, 29 (1998).
[16] F. Chazarenc, G. Merlin, and Y. Gonthier, Ecol. Eng. **21**, 165 (2003).
[17] S. Marsilli-Libelli and N. Checchi, Ecol. Mod. **187**, 201 (2005).
[18] D. Ascuntar, A.F. Toro, M.R. Peña, and C.A. Madera, Ecol. Eng. **35**, 274 (2009).
[19] R.C. Jamieson, T.S. Jamieson, R.J. Gordon, G.W. Stratton, and A. Madani, presented at the 2nd International Wetlands and Remediation Conference, Burlington, Vermont, USA, 2001 (unpublished).
[20] J.E. Gilley, S.C. Finkner, J.W. Doran, and E.R. Kottwitz, App. Eng. Agr. **6**, 35 (1990).
[21] A.Y.C. Lin, J.F. Debroux, J.A. Cunningham, and M. Reinhard, Ecol. Eng. **20**, 75 (2003).
[22] H.J. Bavor, D.J. Roser, S.A. McKersie, and P. Breen, Report to Sydney Water Board, Sydney, NSW, Australia (1988).
[23] M.E. Grismer, Water Environ. Res. **77**, 3047 (2005).
[24] R. Samsó, A. Pedescoll and J. García, presented at the 3rd Wetland Pollutant Dynamics and Control Symposium, Barcelona, Spain, 2009 (unpublished).
[25] J. Kjellin, A. Wörman, H. Johansson, and A. Lindahl, Adv. Water Resources **30**, 838 (2007).
[26] J. Mena, R. Gómez, J. Villaseñor, and A. De Lucas, Can. J. Civ. Eng. **36**, 690 (2009).
[27] G.A. Jenkins and M. Greenway, Ecol. Eng. **25**, 61 (2005).